

A Latent Source Model for Patch-Based Image Segmentation

George H. Chen, Devavrat Shah, and Polina Golland

Massachusetts Institute of Technology, Cambridge MA 02139, USA

Abstract. Despite the popularity and empirical success of patch-based nearest-neighbor and weighted majority voting approaches to medical image segmentation, there has been no theoretical development on when, why, and how well these nonparametric methods work. We bridge this gap by providing a theoretical performance guarantee for nearest-neighbor and weighted majority voting segmentation under a new probabilistic model for patch-based image segmentation. Our analysis relies on a new local property for how similar nearby patches are, and fuses existing lines of work on modeling natural imagery patches and theory for nonparametric classification. We use the model to derive a new patch-based segmentation algorithm that iterates between inferring local label patches and merging these local segmentations to produce a globally consistent image segmentation. Many existing patch-based algorithms arise as special cases of the new algorithm.

1 Introduction

Nearest-neighbor and weighted majority voting methods have been widely used in medical image segmentation, originally at the pixel or voxel level [11] and more recently for image patches [2, 6, 10, 12]. Perhaps the primary reason for the popularity of these nonparametric methods is that standard label fusion techniques for image segmentation require robust nonrigid registration whereas patch-based methods sidestep nonrigid image alignment altogether. Thus, patch-based approaches provide a promising alternative to registration-based methods for problems that present alignment challenges, as in the case of whole body scans or other applications characterized by large anatomical variability.

A second reason for patch-based methods' growing popularity lies in their efficiency of computation: fast approximate nearest-neighbor search algorithms, tailored for patches [3] and for high-dimensional spaces more generally (e.g., [1, 9]), can rapidly find similar patches, and can readily parallelize across search queries. For problems where the end goal is segmentation or a decision based on segmentation, solving numerous nonrigid registration subproblems required for standard label fusion could be a computationally expensive detour that, even if successful, might not produce better solutions than a patch-based approach.

Many patch-based image segmentation methods can be viewed as variations of the following simple algorithm. To determine whether a pixel in the new image should be foreground (part of the object of interest) or background, we consider

the patch centered at that pixel. We compare this image patch to patches in a training database, where each training patch is labeled either foreground or background depending on the pixel at the center of the training patch. We transfer the label from the closest patch in the training database to the pixel of interest in the new image. A plethora of embellishments improve this algorithm, such as, but not limited to, using K nearest neighbors or weighted majority voting instead of only the nearest neighbor [6, 10, 12], incorporating hand-engineered or learned feature descriptors [12], cleverly choosing the shape of a patch [12], and enforcing consistency among adjacent pixels by assigning each training intensity image patch to a label patch rather than a single label [10, 12], or by employing a Markov random field [7].

Despite the broad popularity and success of nonparametric patch-based image segmentation and the smorgasbord of tricks to enhance its performance, the existing work has been empirical with no theoretical justification for when and why such methods should work and, if so, how well and with how much training data. In this paper, we bridge this gap between theory and practice for nonparametric patch-based image segmentation algorithms. We propose a probabilistic model for image segmentation that draws from recent work on modeling natural imagery patches [13, 14]. We begin in Section 2 with a simple case of our model that corresponds to inferring each pixel’s label separately from other pixels. For this special case of so-called pointwise segmentation, we provide a theoretical performance guarantee for patch-based nearest-neighbor and weighted majority voting segmentation in terms of the available training data. Our analysis borrows from existing theory on nonparametric time series classification [5] and crucially relies on a new structural property on neighboring patches being sufficiently similar. We present our full model in Section 3 and derive a new iterative patch-based image segmentation algorithm that combines ideas from patch-based image restoration [13] and distributed optimization [4]. This algorithm alternates between inferring label patches separately and merging these local estimates to form a globally consistent segmentation. We show how various existing patch-based algorithms are special cases of this new algorithm.

2 Pointwise Segmentation and a Theoretical Guarantee

For an image A , we use $A(i)$ to denote the value of image A at pixel i , and $A[i]$ to denote the patch of image A centered at pixel i based on a pre-specified patch shape; $A[i]$ can include feature descriptors in addition to raw intensity values. Each pixel i belongs to a finite, uniformly sampled lattice \mathcal{I} .

Model. Given an intensity image Y , we infer its label image L that delineates an object of interest in Y . In particular, for each pixel $i \in \mathcal{I}$, we infer label $L(i) \in \{+1, -1\}$, where $+1$ corresponds to foreground (object of interest) and -1 to background. We make this inference using patches of image Y , each patch of dimensionality d (e.g., for 2D images and 5-by-5 patches, $d = 5^2 = 25$). We model the joint distribution $p(L(i), Y[i])$ of label $L(i)$ and image patch $Y[i]$ as a generalization of a Gaussian mixture model (GMM) with diagonal covariances, where

each mixture component corresponds to either $L(i) = +1$ or $L(i) = -1$. We define this generalization, called a *diagonal sub-Gaussian mixture model*, shortly.

First, we provide a concrete example where label $L(i)$ and patch $Y[i]$ are related through a GMM with \mathcal{C}_i mixture components. Mixture component $c \in \{1, \dots, \mathcal{C}_i\}$ occurs with probability $\rho_{ic} \in [0, 1]$ and has mean vector $\mu_{ic} \in \mathbb{R}^d$ and label $\lambda_{ic} \in \{+1, -1\}$. In this example, we assume that all covariance matrices are $\sigma^2 \mathbf{I}_{d \times d}$, and that there exists constant $\rho_{\min} > 0$ such that $\rho_{ic} \geq \rho_{\min}$ for all i, c . Thus, image patch $Y[i]$ belongs to mixture component c with probability ρ_{ic} , in which case $Y[i] = \mu_{ic} + W_i$, where vector $W_i \in \mathbb{R}^d$ consists of white Gaussian noise with variance σ^2 , and $L(i) = \lambda_{ic}$. Formally,

$$p(L(i), Y[i]) = \sum_{c=1}^{\mathcal{C}_i} \rho_{ic} \mathcal{N}(Y[i]; \mu_{ic}, \sigma^2 \mathbf{I}_{d \times d}) \delta(L(i) = \lambda_{ic}),$$

where $\mathcal{N}(\cdot; \mu, \Sigma)$ is a Gaussian density with mean μ and covariance Σ , and $\delta(\cdot)$ is the indicator function.

The *diagonal sub-Gaussian mixture model* refers to a generalization where noise vector W_i consists of zero-mean i.i.d. random entries whose distribution has tails that decay at least as fast as that of a Gaussian random variable. Formally, a zero-mean random variable X is sub-Gaussian with parameter σ if its moment generating function $\mathbb{E}[e^{sX}]$ satisfies $\mathbb{E}[e^{sX}] \leq e^{s^2 \sigma^2 / 2}$ for all $s \in \mathbb{R}$. Examples of such random variables include $\mathcal{N}(0, \sigma^2)$ and $\text{Uniform}[-\sigma, \sigma]$.

Every pixel is associated with its own diagonal sub-Gaussian mixture model whose parameters $(\rho_{ic}, \mu_{ic}, \lambda_{ic})$ for $c = 1, \dots, \mathcal{C}_i$ are fixed but unknown. Similar to recent work on modeling generic natural image patches [13, 14], we do not model how different overlapping patches behave jointly and instead only model how each individual patch, viewed alone, behaves. We suspect that medical image patches have even more structure than generic natural image patches, which are very accurately modeled by a GMM [14].

Rather than learning the mixture model components, we instead take a nonparametric approach, using available training data in nearest-neighbor or weighted majority voting schemes to infer label $L(i)$ from image patch $Y[i]$. To this end, we assume we have access to n i.i.d. training intensity-label *image* pairs $(Y_1, L_1), \dots, (Y_n, L_n)$ that obey our probabilistic model above.

Inference. We consider two simple segmentation methods that operate on each pixel i separately, inferring label $L(i)$ only based on image patch $Y[i]$.

Pointwise nearest-neighbor segmentation first finds which training intensity image Y_u has a patch centered at pixel j that is closest to observed patch $Y[i]$. This amounts to solving $(\hat{u}, \hat{j}) = \operatorname{argmin}_{u \in \{1, 2, \dots, n\}, j \in N(i)} \|Y_u[j] - Y[i]\|^2$, where $\|\cdot\|$ denotes Euclidean norm, and $N(i)$ refers to a user-specified finite set of pixels that are neighbors of pixel i . Label $L(i)$ is estimated to be $L_{\hat{u}}(\hat{j})$.

Pointwise weighted majority voting segmentation first computes the following weighted votes for labels $\ell \in \{+1, -1\}$:

$$V_\ell(i|Y[i]; \theta) \triangleq \sum_{u=1}^n \sum_{j \in N(i)} \exp(-\theta \|Y_u[j] - Y[i]\|^2) \delta(L_u(j) = \ell),$$

where θ is a scale parameter, and $N(i)$ again refers to user-specified neighboring pixels of pixel i . Label $L(i)$ is estimated to be the label ℓ with the higher vote $V_\ell(i|Y[i]; \theta)$. Pointwise nearest-neighbor segmentation can be viewed as this weighted voting with $\theta \rightarrow \infty$. Pointwise weighted majority voting has been used extensively for patch-based segmentation [2, 6, 10, 12], where we note that our formulation readily allows for one to choose which training image patches are considered neighbors, what the patch shape is, and whether feature descriptors are part of the intensity patch vector $Y[i]$.

Theoretical guarantee. The model above allows nearby pixels to be associated with dramatically different mixture models. However, real images are “smooth” with patches centered at two adjacent pixels likely similar. We incorporate this smoothness via a structural property on the sub-Gaussian mixture model parameters associated with nearby pixels. We refer to this property as the *jigsaw condition*, which holds if for every mixture component $(\rho_{ic}, \mu_{ic}, \lambda_{ic})$ of the diagonal sub-Gaussian mixture model associated with pixel i , there exists a neighbor $j \in N^*(i)$ such that the diagonal sub-Gaussian mixture model associated with pixel j also has a mixture component with mean μ_{ic} , label λ_{ic} , and mixture weight at least ρ_{\min} ; this weight need not be equal to ρ_{ic} . The shape and size of neighborhood $N^*(i)$, which is fixed and unknown, control how similar the mixture models are across image pixels. Note that $N^*(i)$ affects how far from pixel i we should look for training patches, i.e., how to choose neighborhood $N(i)$ in pointwise nearest-neighbor and weighted majority voting segmentation, where ideally $N(i) = N^*(i)$.

Separation gap. Our theoretical result also depends on the separation “gap” between training intensity image patches that correspond to the two different labels:

$$\mathcal{G} \triangleq \min_{\substack{u,v \in \{1,\dots,n\}, \\ i \in \mathcal{I}, j \in N(i) \text{ s.t. } L_u(i) \neq L_v(j)}} \|Y_u[i] - Y_v[j]\|^2.$$

Intuitively, a small separation gap corresponds to the case of two training intensity image patches that are very similar but one corresponds to foreground and the other to background. In this case, a nearest-neighbor approach may easily select a patch with the wrong label, resulting in an error.

We now state our main theoretical guarantee. The proof is left to the supplementary material and builds on existing time series classification analysis [5].

Theorem 1. *Under the model above with n training intensity-label image pairs and provided that the jigsaw condition holds with neighborhood N^* , pointwise nearest-neighbor and weighted majority voting segmentation (with user-specified neighborhood N satisfying $N(i) \supseteq N^*(i)$ for every pixel i and with parameter $\theta = \frac{1}{8\sigma^2}$ for weighted majority voting) achieve expected pixel labeling error rate*

$$\mathbb{E} \left[\frac{1}{|\mathcal{I}|} \sum_{i \in \mathcal{I}} \delta(\text{mislabel pixel } i) \right] \leq |\mathcal{I}| C_{\max} \exp \left(-\frac{n\rho_{\min}}{8} \right) + |N|n \exp \left(-\frac{\mathcal{G}}{16\sigma^2} \right),$$

where C_{\max} is the maximum number of mixture components of any diagonal sub-Gaussian mixture model associated with a pixel, and $|N|$ is the largest user-specified neighborhood of any pixel.

To interpret this theorem, we consider sufficient conditions for each term on the right-hand side bound to be at most $\varepsilon/2$ for $\varepsilon \in (0, 1)$. For the first term, the number of training intensity-label image pairs n should be sufficiently large so that we see all the different mixture model components in our training data: $n \geq \frac{8}{\rho_{\min}} \log(2|\mathcal{I}|\mathcal{C}_{\max}/\varepsilon)$. For the second term, the gap \mathcal{G} should be sufficiently large so that the nearest training intensity image patch found does not produce a segmentation error: $\mathcal{G} \geq 16\sigma^2 \log(2|N|n/\varepsilon)$. There are different ways to change the gap, such as changing the patch shape and including hand-engineered or learned patch features. Intuitively, using larger patches d should widen the gap, but using larger patches also means that the maximum number of mixture components \mathcal{C}_{\max} needed to represent a patch increases, possibly quite dramatically.

The dependence on n in the second term results from a worst-case analysis. To keep the gap from having to grow as $\log(n)$, we could subsample the training data so that n is large enough to capture the diversity of mixture model components yet not so large that it overcomes the gap. In particular, treating \mathcal{C}_{\max} , σ^2 , and ρ_{\min} as constants that depend on the application of interest and could potentially be estimated from data, collecting $n = \Theta(\log(|\mathcal{I}|/\varepsilon))$ training image pairs and with a gap $\mathcal{G} = \Omega(\log((|N| \log |\mathcal{I}|)/\varepsilon))$, both algorithms achieve an expected error rate of at most ε . The intuition is that as n grows large, if we continue to consider all training subjects, even those that look very different from the new subject, we are bound to get unlucky (due to noise in intensity images) and, in the worst case, encounter a training image patch that is close to a test image patch but has the wrong label. Effectively, outliers in training data muddle nearest-neighbor inference, and more training data means possibly more outliers.

3 Multipoint Segmentation

Model. We generalize the basic model to infer label patches $L[i]$ rather than just a single pixel’s label $L(i)$. Every label patch $L[i]$ is assumed to have dimensionality d' , where d and d' need not be equal. For example, for 2D images, $Y[i]$ could be a 5-by-5 patch ($d = 25$) whereas $L[i]$ could be a 3-by-3 patch ($d' = 9$). When $d' > 1$, estimated label patches must be merged to arrive at a globally consistent estimate of label image L . This case is referred to as multipoint segmentation.

In this general case, we assume there to be k latent label images A_1, \dots, A_k that occur with probabilities π_1, \dots, π_k . To generate intensity image Y , we first sample label image $A \in \{A_1, \dots, A_k\}$ according to probabilities π_1, \dots, π_k . Then we sample label image L to be a perturbed version of A such that $p(L|A) \propto \exp(-\alpha \mathbf{d}(L, A))$ for some constant $\alpha \geq 0$ and differentiable “distance” function $\mathbf{d}(\cdot, \cdot)$. For example, $\mathbf{d}(L, A)$ could relate to volume overlap between the segmentations represented by label images L and A with perfect overlap yielding distance 0. Finally, intensity image Y is generated so that for each pixel $i \in \mathcal{I}$, patch $Y[i]$ is a sample from a mixture model patch prior $p(Y[i]|L[i])$. If $\alpha = 0$, $d' = 1$, and the mixture model is diagonal sub-Gaussian, we get our earlier model.

We refer to this formulation as a *latent source model* since the intensity image patches could be thought of as generated from the latent “canonical” label

images A_1, \dots, A_k combined with the latent mixture model clusters linking label patches $L[i]$ to intensity patches $Y[i]$. This hierarchical structure enables local appearances around a given pixel to be shared across the canonical label images.

Inference. We outline an iterative algorithm based on the expected patch log-likelihood (EPLL) framework [13], deferring details to the supplementary material. The EPLL framework seeks a label image L by solving

$$\hat{L} = \operatorname{argmax}_{L \in \{+1, -1\}^{|\mathcal{I}|}} \left\{ \log \left(\sum_{g=1}^k \pi_g \exp(-\alpha \mathbf{d}(L, A_g)) \right) + \frac{1}{|\mathcal{I}|} \sum_{i \in \mathcal{I}} \log p(Y[i]|L[i]) \right\}.$$

The first term in the objective function encourages label image L to be close to the true label images A_1, \dots, A_k . The second term is the ‘‘expected patch log-likelihood’’, which favors solutions whose local label patches agree well on average with the local intensity patches according to the patch priors. Since latent label images A_1, \dots, A_k are unknown, we use training label images L_1, \dots, L_n as proxies instead, replacing the first term in the objective function with $F(L; \alpha) \triangleq \log \left(\frac{1}{n} \sum_{u=1}^n \exp(-\alpha \mathbf{d}(L, L_u)) \right)$. Next, we approximate the unknown patch prior $p(Y[i]|L[i])$ with a kernel density estimate

$$\tilde{p}(Y[i]|L[i]; \gamma) \propto \sum_{u=1}^n \sum_{j \in N(i)} \mathcal{N} \left(Y[i]; Y_u[j], \frac{1}{2\gamma} \mathbf{I}_{d \times d} \right) \delta(L[i] = L_u[j]),$$

where the user specifies a neighborhood $N(i)$ of pixel i , and constant $\gamma > 0$ that controls the Gaussian kernel’s bandwidth. We group the pixels so that nearby pixels within a small block all share the same kernel density estimate. This approximation assumes a stronger version of the jigsaw condition from Section 2 since the algorithm operates as if nearby pixels have the same mixture model as a patch prior. We thus maximize objective $F(L; \alpha) + \frac{1}{|\mathcal{I}|} \sum_{i \in \mathcal{I}} \log \tilde{p}(Y[i]|L[i]; \gamma)$.

Similar to the original EPLL method [13], we introduce an auxiliary variable $\xi_i \in \mathbb{R}^d$ for each patch $L[i]$, where ξ_i acts as a local estimate for $L[i]$. Whereas two patches $L[i]$ and $L[j]$ that overlap in label image L must be consistent across the overlapping pixels, there is no such requirement on their local estimates ξ_i and ξ_j . In summary, we maximize the objective $F(L; \alpha) + \frac{1}{|\mathcal{I}|} \sum_{i \in \mathcal{I}} \log \tilde{p}(Y[i]|\xi_i; \gamma) - \frac{\beta}{2} \sum_{i \in \mathcal{I}} \|L[i] - \xi_i\|^2$ for $\beta > 0$, subject to constraints $L[i] = \xi_i$ that are enforced using Lagrange multipliers. We numerically optimize this cost function using the Alternating Direction Method of Multipliers for distributed optimization [4]. Given the current estimate of label image L , the algorithm produces estimate ξ_i for $L[i]$ given $Y[i]$ in parallel across i . Next, it updates L based on ξ_i via a gradient method. Finally, the Lagrange multipliers are updated to penalize large discrepancies between ξ_i and $L[i]$.

Fixing ξ_i and updating L corresponds to merging local patch estimates to form a globally consistent segmentation. This is the only step that involves expression $F(L; \alpha)$. With $\alpha = 0$ and forcing the Lagrange multipliers to always be zero, the merging becomes a simple averaging of overlapping label patch estimates ξ_i . This algorithm corresponds to existing multipoint patch-based segmentation algorithms [6, 10, 12] and the in-painting technique achieved by the

original EPLL method. Setting $\alpha = \beta = 0$ and $d' = 1$ yields pointwise weighted majority voting with parameter $\theta = \gamma$. When $\alpha > 0$, a global correction is applied, shifting the label image estimate closer to the training label images. This should produce better estimates when the full training label images can, with small perturbations as measured by $\mathbf{d}(\cdot, \cdot)$, explain new intensity images.

Experimental results. We empirically explore the new iterative algorithm on 20 labeled thoracic-abdominal contrast-enhanced CT scans from the Visceral ANATOMY3 dataset [8]. We train the model on 15 scans and test on the remaining 5 scans. The training procedure amounted to using 10 of the 15 training scans to estimate the algorithm parameters in an exhaustive sweep, using the rest of the training scans to evaluate parameter settings. Finally, the entire training dataset of 15 scans is used to segment the test dataset of 5 scans using the best parameters found during training. For each test scan, we first use a fast affine registration to roughly align each training scan to the test scan. Then we apply four different algo-

rithms: a baseline majority voting algorithm (denoted “MV”) that simply averages the training label images that are now roughly aligned to the test scan, pointwise nearest neighbor (denoted “1NN”) and weighted majority voting (denoted “WMV”) segmentation that both use approximate nearest patches, and finally our proposed iterative algorithm (denoted “ADMM”), setting distance \mathbf{d} to one minus Dice overlap. Note that Dice overlap can be reduced to a differentiable function by relaxing our optimization to allow each label to take on a value in $[-1, 1]$. By doing so, the Dice overlap of label images L and A is given by $2\langle \tilde{L}, \tilde{A} \rangle / (\langle \tilde{L}, \tilde{L} \rangle + \langle \tilde{A}, \tilde{A} \rangle)$, where $\tilde{L} = (L + 1)/2$ and $\tilde{A} = (A + 1)/2$.

We segmented the liver, spleen, left kidney, and right kidney. We report Dice overlap scores for the liver in Fig. 1 using the four algorithms. Our results for segmenting the other organs follow a similar trend where the proposed algorithm outperforms pointwise weighted majority voting, which outperforms both pointwise nearest-neighbor segmentation and the baseline majority voting. For the organs segmented, there was little benefit to having $\alpha > 0$, suggesting the local patch estimates to already be quite consistent and require no global correction.

4 Conclusions

We have established a new theoretical performance guarantee for two nonparametric patch-based segmentation algorithms, uniting recent lines of work on modeling patches in natural imagery and on theory for nonparametric time series classification. Our result indicates that if nearby patches behave as mixture models with sufficient similarity, then a myopic segmentation works well, where its quality is stated in terms of the available training data. Our main performance bound provides insight into how one should approach building a training dataset

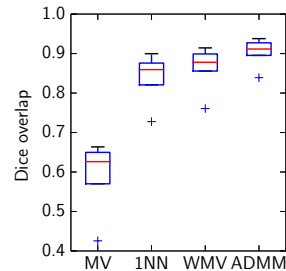


Fig. 1. Liver segmentation results.

for patch-based segmentation. The looseness in the bound could be attributed to outliers in training data. Detecting and removing these outliers should lead to improved segmentation performance.

From a modeling standpoint, understanding the joint behavior of patches could yield substantial new insights into exploiting macroscopic structure in images rather than relying only on local properties. In a related direction, while we have modeled the individual behavior of patches, an interesting theoretical problem is to find joint distributions on image pixels that lead to such marginal distributions on patches. Do such joint distributions exist? If not, is there a joint distribution whose patch marginals approximate the mixture models we use? These questions outline rich areas for future research.

Acknowledgments. This work was supported in part by the NIH NIBIB NAC P41EB015902 grant, MIT Lincoln Lab, and Wistron Corporation. GHC was supported by an NDSEG fellowship.

References

1. N Ailon and B Chazelle. Approximate nearest neighbors and the fast johnson-lindenstrauss transform. In *Symposium on Theory of Computing*, 2006.
2. W Bai et al. A probabilistic patch-based label fusion model for multi-atlas segmentation with registration refinement: Application to cardiac MR images. *Transactions in Medical Imaging*, 2013.
3. C Barnes et al. Patchmatch: a randomized correspondence algorithm for structural image editing. *Transactions on Graphics*, 2009.
4. S Boyd et al. Distributed optimization and statistical learning via the alternating direction method of multipliers. *Foundations & Trends in Machine Learning*, 2011.
5. G H Chen, S Nikolov, and D Shah. A latent source model for nonparametric time series classification. In *Neural Information Processing Systems*, 2013.
6. P Coupé et al. Patch-based segmentation using expert priors: Application to hippocampus and ventricle segmentation. *NeuroImage*, 2011.
7. W T Freeman and C Liu. Markov random fields for super-resolution and texture synthesis. *Advances in Markov Random Fields for Vision and Image Proc.*, 2011.
8. A Hanbury, H Müller, G Langs, M A Weber, B H Menze, and T Salas Fernandez. Bringing the algorithms to the data: Cloud-based benchmarking for medical image analysis. In T Catarci, P Forner, D Hiemstra, A Peñas, and G Santucci, editors, *CLEF Conference*, volume 7488 of *LNCS*, pages 24–29. Springer, Heidelberg, 2012.
9. M Muja and D G Lowe. Fast approximate nearest neighbors with automatic algorithm configuration. In *ICCVTA*, 2009.
10. F Rousseau, P A Habas, and C Studholme. A supervised patch-based approach for human brain labeling. *Transactions on Medical Imaging*, 2011.
11. M R Sabuncu et al. A generative model for image segmentation based on label fusion. *Transactions on Medical Imaging*, 2010.
12. C Wachinger et al. On the importance of location and features for the patch-based segmentation of parotid glands. *MIDAS Journal - IGART*, 2014.
13. D Zoran and Y Weiss. From learning models of natural image patches to whole image restoration. In *International Conference on Computer Vision*, 2011.
14. D Zoran and Y Weiss. Natural images, gaussian mixtures and dead leaves. In *Neural Information Processing Systems*, 2012.